



Spatial evolution of laser filaments in turbulent air

Tao Zeng^a, Shiping Zhu^{b,*}, Shengling Zhou^b, Yan He^b

^a School of Physical Science and Technology, Southwest University, 400715 Chongqing, China

^b College of Engineering and Technology, Southwest University, 400716 Chongqing, China



ARTICLE INFO

Keywords:

Ultrafast phenomena
Atmospheric propagation
Atmospheric turbulence

ABSTRACT

In this study, the spatial evolution properties of laser filament clusters in turbulent air were evaluated using numerical simulations. Various statistical parameters were calculated, such as the percolation probability, filling factor, and average cluster size. The results indicate that turbulence-induced multi-filamentation can be described as a new phase transition universality class. In addition, during this process, the relationship between the average cluster size and filling factor could be fit by a power function. Our results are valuable for applications involving filamentation that can be influenced by the geometrical features of multiple filaments.

© 2017 Elsevier B.V. All rights reserved.

1. Introduction

Currently, femtosecond laser filaments have attracted extensive research interest because of their promising applications, such as atmospheric remote sensing [1,2], lightning control [3,4], rain production [5,6], and terahertz (THz) wave generation [7,8]. Considering the influence of atmospheric turbulence on the filament propagation properties, numerous experimental and theoretical studies have been conducted on turbulence-induced filament wandering [9–14] and multiple filament formation [15–17].

The multi-filamentation phenomenon is commonly caused by transverse modulational instability, resulting from small perturbations in the initial laser beam profile or inhomogeneities in the optical media refractive index. It has been demonstrated that a strong enhancement in radiated THz energy can be obtained by multiple filaments with the presence of a static electric field [18]. In addition, many atmospheric applications such as laser-induced condensation or lightning triggering rely on the connectivity between multiple filaments [19]. Nevertheless, the structural evolution features of multiple filaments induced by air turbulence have not yet been clarified. It has recently been demonstrated that the onset of multi-filamentation resulting from an initially noisy input beam profile could be described as a critical phenomenon and a new phase transition universality class [19]. These findings will provide an effective method to study the evolution of filament clusters induced by air turbulence from the viewpoint of phase transitions.

In this work, we investigate the spatial distribution of multiple filaments under the condition of air turbulence using numerical simulations. We found that the evolution of the filament clusters exhibits

phase transitions. Moreover, it has been characterized by a series of parameters such as the percolation probability, filling factor, and average cluster size. Our results could be valuable for applications involving filamentation in the atmosphere that can be influenced by the geometrical features of multiple filaments.

2. Numerical simulation model

Numerical simulations of filamentation in turbulent air were carried out according to the 2D + 1 (x, y, z) nonlinear wave equation, which describes the nonlinear propagation of a continuous wave (CW) beam in turbulent air:

$$2ik_0 \frac{\partial A}{\partial z} + \left(\frac{\partial^2}{\partial x^2} + \frac{\partial^2}{\partial y^2} \right) A + 2k_0^2 \Delta n A + 2k_0^2 \tilde{n}(x, y, z) A = 0. \quad (1)$$

Here, $A(x, y, z)$ is the amplitude of the laser field. Insofar as we focused exclusively on the spatial distribution of filament propagation in turbulent air, the temporal aspect of the light field was not considered in the simulation. In addition, the validity of this model has been demonstrated in previous studies [20,21]. Here, k_0 represents the wave number of the 800-nm laser beam in our simulation, and Δn represents the nonlinear refractive index induced by the optical Kerr effect ($\Delta n_{ker} = n_2 I, n_2 = 2 \times 10^{-19} \text{ cm}^2/\text{W}$) and the effective counteracting higher-order nonlinear refractive index of the plasma defocusing effect ($\Delta n_{plasma} = -\sigma I^m, m = 8$) [22]. Further, I denotes the laser intensity and σ is an empirical parameter corresponding to a clamped intensity of $5.0 \times 10^{13} \text{ W/cm}^2$ [21]. Finally, $\tilde{n}(x, y, z)$ represents the fluctuations in the refractive index

* Corresponding author.

E-mail addresses: taozeng@swu.edu.cn (T. Zeng), zpswu@126.com (S. Zhu).

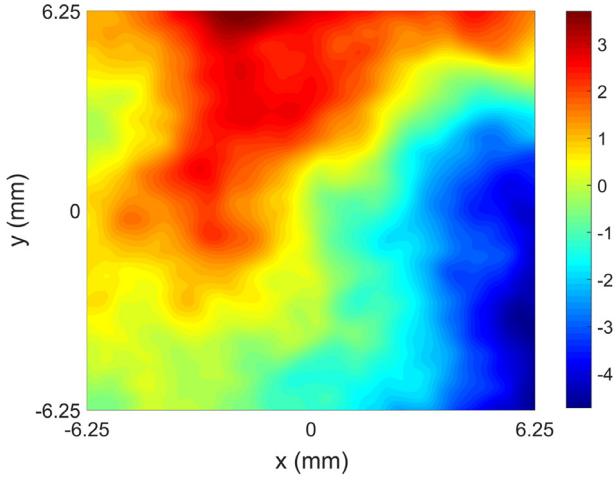


Fig. 1. Representative turbulence phase screen with structure constant $C_n^2 = 10^{-11} \text{ cm}^{-2/3}$ and propagation distance $\Delta z = 1 \text{ m}$. The outer and inner scales are $L_0 = 1 \text{ m}$ and $l_0 = 1 \text{ mm}$, respectively.

of air induced by atmospheric turbulence and can be obtained based on the turbulence phase screen model as follows.

The refractive index fluctuations resulting from a stationary, homogeneous, and isotropic turbulence flow field can be described by the modified Karman spectrum [11,17]:

$$F_n(\kappa_x, \kappa_y, \kappa_z) = 0.033C_n^2(\kappa^2 + \kappa_0^2)^{-11/6} \exp\left[-(\kappa/\kappa_m)^2\right], \quad (2)$$

where C_n^2 is the refractive index structure constant, which determines the fluctuation intensity of the refractive index of air. κ represents the spatial wave number and has three vertical components, κ_x , κ_y , and κ_z , while $\kappa_0 = 2\pi/L_0$ and $\kappa_m = 5.92/l_0$. L_0 and l_0 represent the outer and inner scales of the air turbulence, respectively. Then, we derive a series of turbulence phase screens denoted by $\phi(x, y)$ that represent the cumulative phase shift within the beam propagation distance Δz based on Eq. (2), according to the method used in previous studies [23,24]. In our simulation, C_n^2 was selected to be $10^{-11} \text{ cm}^{-2/3}$ which refers to relatively strong turbulence near the ground [25]. Moreover, L_0 and l_0 are 1 m and 1 mm, respectively, and Δz is 1 m, corresponding to the outer scale of the turbulence. When the refractive index structure constant C_n^2 of air turbulence is not strong enough, such as in Ref. [12] with C_n^2 of $1.4 \times 10^{-14} \text{ cm}^{-2/3}$, the turbulence would only lead to the single filament wandering and multiple filaments would not be generated. As we mainly focused on the spatial evolution of multiple filaments, a relative strong turbulence was used to guarantee the occurrence of multiple filaments.

Fig. 1 shows a representative turbulence phase screen obtained with the above turbulence parameters. The accuracy of the turbulence phase screen was verified based on the theoretical phase structure function [26]. Finally, we obtain the fluctuations in the refractive index of air $\tilde{n}(x, y, z)$ from the following equation:

$$\tilde{n}(x, y, z) = \frac{\phi(x, y)}{k_0 \Delta z}. \quad (3)$$

Temporal effects including self-steeping, group-velocity dispersion effect, multiphoton absorption effect, and turbulence temporal variation were neglected in our simulation model. This kind of simplification would significantly influence the temporal dynamics of laser pulse. However, to a lesser extent it would influence the spatial evolution of laser filaments in principle, which is clarified in the following three points.

Firstly, we neglected the temporal terms associated with self-steeping and dispersion effect in Eq. (1). Generally, the filament radius a in air is about $40 \mu\text{m}$. The corresponding longitudinal scale of spatial

transformation a^2 is about 1.26 cm. Moreover, the second order group-velocity dispersion coefficient k'' for air is $0.2 \text{ fs}^2/\text{cm}$ [27]. For femtosecond laser pulse with duration τ of 20 fs, the characteristic dispersion length scale τ^2/k'' of the temporal changes is about 20 m, which is much longer than the spatial transformation scale. Therefore, the spatial effects develop much faster than the temporal effects and dominate the multiple filamentation dynamics [27]. As the laser intensity remains constant due to intensity-clamping effect of filament, the change of peak intensity will not influence spatial evolution feature of filament clusters. In addition, for laser pulse with low initial power, the back part energy of the pulse would be diffracted out and constitute part of the background reservoir. For laser pulse with relative strong initial power, the back part of the pulse would form a ring caused by diffraction effect. Then the hot spot in the ring contains enough power comparing to the critical power tend to produce new filament. For very high input laser power such as in our simulation, the new filaments will go into a disordered regime. A CW laser beam with high input power will also form a ring induced by plasma diffraction effect and evolve with the same dynamic process under our simulation conditions.

Secondly, the multiphoton absorption process was not considered in Eq. (1). As the multiphoton absorption effect results in the pulse energy loss, it would influence the filament length finally and have little effect on the spatial evolution of filaments. Moreover, in our simulation experiment it is supposed that the filament length is long enough for the filament propagation in the turbulent air within a distance of 5 m.

Thirdly, the turbulence temporal variation was also neglected in our simulation model. The shot-to-shot motion driven by air turbulence is at millisecond timescale [17], which is many orders magnitudes longer than the laser pulse duration. Therefore, this simplification of turbulence model is also reasonable.

In this work, we simulated the propagation of a CW symmetrical Gaussian laser beam with an initial radius W_0 ($1/e^2$) of 2.5 mm under the turbulent atmospheric condition. The input laser power P_{in} is as high as 4.7 GW, corresponding to approximately 100 P_{cr} . Here, P_{cr} represents the critical laser power in air, leading to the appearance of a filament under the dynamic interaction between diffraction and self-focusing. Then, the estimated self-focusing distance without turbulence is approximately 100 cm according to the following equation [28,29]:

$$z_f = \frac{0.367\pi/\lambda W_0^2}{\sqrt{\left[(P_{in}/P_{cr})^{1/2} - 0.852\right]^2 - 0.0219}}. \quad (4)$$

3. Results and discussion

To study the statistical regularities of multiple filaments, we performed 63 independent simulations of multiple filament propagation in turbulent air by using a different series of stochastic turbulence phase screens for each simulation. The turbulence was introduced in the whole propagation process of the laser beam. Thus the first turbulence screen was placed at the beginning propagation point of the initial symmetrical Gaussian laser beam. Each screen from the same series was inserted in the propagation path for every 1 m. Fig. 2 depicts the laser beam intensity distribution at different distances as a representative simulation result, illustrating the formation of multiple filaments during the nonlinear propagation process in turbulent air for an initial symmetrical Gaussian laser beam. The intensity in each picture has been set to a fixed threshold of $1 \text{ TW}/\text{cm}^2$, which is slightly below the initial beam intensity level.

Regarding cluster evolution, only a single cluster pattern can be seen in Figs. 2(a)–(c). With the increase in propagation distance, the cluster structure becomes increasingly asymmetrical, owing to the turbulence-induced modulation instability of the wave front. During the self-focusing process, the maximum laser intensity on the cross-section increases gradually with the distance and reaches a clamped intensity of approximately $5.0 \times 10^{13} \text{ W}/\text{cm}^2$ at a distance of around 140 cm.

Download English Version:

<https://daneshyari.com/en/article/7925948>

Download Persian Version:

<https://daneshyari.com/article/7925948>

[Daneshyari.com](https://daneshyari.com)